Journal of Groundwater Science and Engineering
ISSN 2305-7068
Indexed by ESCI CABI CSA
Scopus GeoRef AJ CNKI

Delineation of groundwater potential zones in Wadi Saida Watershed of NW-Algeria using remote sensing, geographic information system-based AHP techniques and geostatistical analysis

Cherif Kessar, Yamina Benkesmia, Bilal Blissag, Lahsen Wahib Kébir

Citation:
Cherif Kessar, Yamina Benkesmia, Bilal Blissag, Lahsen Wahib Kébir. Delineation of groundwater potential zones in Wadi Saida Watershed of NW-Algeria using remote sensing, geographic information system-based AHP techniques and geostatistical analysis[J]. *Journal of Groundwater Science and Engineering*, 2021, 9(1): 45-64.

View online: https://doi.org/10.19637/j.cnki.2305-7068.2021.01.005

DOI: 10.19637/j.cnki.2305–7068.2021.01.005

Delineation of groundwater potential zones in Wadi Saida Watershed of NW-Algeria using remote sensing, geographic information system-based AHP techniques and geostatistical analysis

Cherif Kessar*, Yamina Benkesmia, Bilal Blissag, Lahsen Wahib Kébir

Agence Spatiale Algérienne, Centre des Techniques Spatiales, Arzew, Algérie.

Abstract: Sustainable management of groundwater resources has now become an obligation, especially in arid and semi-arid regions given the socio-economic importance of this resource. The optimization in zoning for groundwater exploitation helps in planning and managing groundwater supply works such as boreholes and wells in the catchment. The objective of this study is to use remote sensing and GIS-based Analytical Hierarchy Process (AHP) techniques to evaluate the groundwater potential of Wadi Saida Watershed. Spatial analysis such as geostatistics was also used to validate results and ensure more accuracy. Through the GIS tools and remote sensing technique, earth observation data were converted into thematic layers such as lineament density, geology, drainage density, slope, land use and rainfall, which were combined to delineate groundwater potential zones. Based on their respective impact on groundwater potential, the AHP approach was adopted to assign weights on multi-influencing factors. These results will enable decision-makers to optimize hydrogeological exploration in large-scale catchment areas and map areas. According to the results, the southern part of the Wadi Saida Watershed is characterized as a higher groundwater potential area, where 32% of the total surface area falls in the excellent and good class of groundwater potential. The validation process revealed a 71% agreement between the estimated and actual yield of the existing boreholes in the study area.

Keywords: Wadi Saida Watershed; Groundwater potential mapping; Remote Sensing; GIS; Analytical Hierarchical Process; Geostatistic

Received: 10 Sep 2020/ Accepted: 03 Dec 2020

Cherif Kessar, Yamina Benkesmia, Bilal Blissag, *et al*. 2021. Delineation of groundwater potential zones in Wadi Saida Watershed of NW-Algeria using remote sensing, geographic information system-based AHP techniques and geostatistical analysis. Journal of Groundwater Science and Engineering, 9(1): 45-64.

Introduction

Groundwater is a dynamic and important replenishable natural freshwater resource (Shekhar and Pandey, 2014). Globally, groundwater represents one-third of all freshwater exploitation, providing an expected 36%, 42%, and 27% of the water used for domestic, agricultural, and industrial purposes respectively (Döell *et al*. 2012). Demand for freshwater resources in the world is critically increasing as a result of rapid growth of industrial activities and population. Consequently, proper groundwater investigation and extraction is now an important part of groundwater management (Senanayake *et al*. 2015). The United Nations Environment Program estimates that more than two billion people will live with high water stress by 2050, which would limit the development of many countries around the world (Sekar and Randhir, 2007). In the last century, global water

*Corresponding author. E-mail: ckessar@cts.asal.dz

use has increased six times and continues to grow by 1% every year attaining 30% by 2050, which is responding to excessive demand related to population growth and economic development (WWDR, 2019). According to Field *et al*. (2014), by 2020, between 75 million and 250 million people in Africa would be exposed to increased water stress, and in some regions, rainfed agriculture yields would be reduced by 50%. Access to food could be severely compromised in such situation.

In Algeria, where the population was estimated at 46 million in 2020, water requirements were estimated at 5 billion m^3/a. The demand for fresh-water grows every year by 4% to 5%, while current mobilization is barely 2 billion m^3/a (Kettab, 2001).

Defined as the amount of groundwater available in an area, groundwater potential is dependent on several hydrological and hydrogeological factors (Gdoura *et al*. 2015). At a different spatial scale, it has become necessary to utilize appropriate new techniques for prospecting groundwater (Le Page *et al*. 2012). Geophysical prospecting and experimental techniques are among the best-known techniques for achieving this goal. However, proper water resource management requires the application of new approaches for decision supporting. Due to the strict policies on groundwater management in semi-arid regions and the high cost of investigations regarding the development of new boreholes, new approaches have been developed and widely used with data availability and result validation. Countless researchers around the world have conducted studies on the applications of remote sensing and GIS for the exploration of groundwater potential areas, and it has been found that the determination of these areas is influenced by the various factors, which needs a consequent validation (Magesh *et al*. 2012) The results are evaluated based on field review and change of geo-environmental conditions. Currently, AHP techniques based on GIS and remote sensing is the most popular approach in mapping groundwater potential areas and several such studies have been conducted in the past years (Pankaj *et al*. 2006; Ould Cherif Ahmed *et al*. 2008; Chowdhury *et al*. 2009; Suja Rose and Krishnan, 2009; Jha *et al*. 2010; Adiat *et al*. 2012; Alaa and Ayseer, 2015; Hachem *et al*. 2015; Rajasekhar *et al*. 2019; Nithyaa *et al*. 2019; Gebru *et al*. 2020; Ghosh *et al*. 2020). The availability of spatial, spectral and temporal remote sensing data provides immediate convenience for studies over large and relatively inaccessible areas. Remote sensing has, therefore, become an adequate method for assessing, monitoring and conserving groundwater resources (Balasubramani, 2018). Such operational challenges remain, until now, the main hindrance for the authorities to make decision on a proper location for groundwater extraction, and solving such difficulties is the main aim of this research, for which a multi-criteria decision-making tool (MCDM) such as analytical hierarchical method (AHP) is employed (Kessar *et al*. 2020).

The AHP, developed by Saaty (1980), offers a strong and readily understood way of evaluating complicated problems (Alaa and Ayser, 2015), to ensures the optimal use of groundwater resources and sustainable management of this wealth. This research aims to build a groundwater potential map of the Wadi Saida Watershed, northwest of Algeria using integrated RS, GIS and AHP techniques. The contribution of this study focuses on the utilization of spatial analysis techniques to visualize, validate and propose areas with good groundwater potential. The heterogeneity of the data from the sources, the hierarchical process and the validation of results using geostatistical analysis of existing boreholes are considered as excellent contributions if the field data are available.

1 Study area

The watershed of Wadi Saida (coded 11-11) is geographically situated between X=223 110, X=250 600 and Y=3 889 100, Y= 3 844 370 (Coordinate system: WGS 84-UTM). It is part of the larger Macta basin, which stretches northwest of Algeria, in the last tabular uplands of the southern side of the Tellian Atlas, composed by the Tlemcen, Daïa and Saida Mountains (Kessar *et al*. 2020), and on the edge of the high steppe plains (Fig. 1). With a surface area of 624.66 km^2, it is located between the ends of the mountains of Daïa in the north and the highlands region in the south. It is limited from the West side by; the Sidi Ahmed Zeggaï Mountain, the Sidi Abdelkader Mountain to the south, the Saida Mountain to the east and the Djebel Tiffrit Mountain, which peak at 1 200 m. The Wadi Saida Watershed is

characterized by semi-arid climate, during the year by two major seasons are observed. A cold season characterized by an average minimum temperature values of 10°C (between December and February), seasonal temperatures drop sometimes below 0°C, resulting in the occurrence of frost. The average monthly temperature (Saida Station) is high between June and September with a maximum of 27.5°C observed in July and August. The average annual potential evaporation is 835 mm (Yles, 2014). The wadi Saida Watershed is subject to the influence of two opposite seasonal regimes. The first is dominated by Mediterranean climate with marine influence causing heavy rainfall in winter. The second is characterized by the storms in the summer season. The analysis of the rainfall series from five available gauging stations (1975-2014) shows that 1997 was the rainiest year with an annual rainfall of 516.12 mm, while the lowest is 199.24 mm in the year of 1999.

The watershed is well drained by a fairly dense hydrographic network, small tributaries arise from high areas and rainwater collects in the valley where it is crossed by the main wadi of Saida. It extends from the north end of the city of Saida, crosses the cities of Rebahia, Sidi Amar and Sidi Boubkeur to arrive at Wadi Taria in Mascara province. The main tributaries are Wadi Massil in the east of Hammam Rabi city, Wadi Nazreg in the east of Rebahia city and Wadi Tebouda crossing Ain el Hadjar in the south of Saida province (Fig. 1). Overall, the surface flow generally follows a northward direction which has an outlet.

The wadi Saida Basin has a complex and diversified geology (Medjber and Berkane, 2016). It is part of the Tlemcenian domain and a subset of the atlasic domain (Fig. 3). The Jurassic formations are the dominant in the study area, in which the Lower Jurassic consist of dolomitized limestones and marls and the Upper Jurassic consists of clays and sandstone limestones. Dolomitic rocks and limestones are generally highly karstified. In the depressions as well as the valleys and wadi beds, lands of continental origin (Fluviatile and Aeolians) of tertiary age are often found and Mio-Pliocene and Quaternary are mostly undifferentiated.

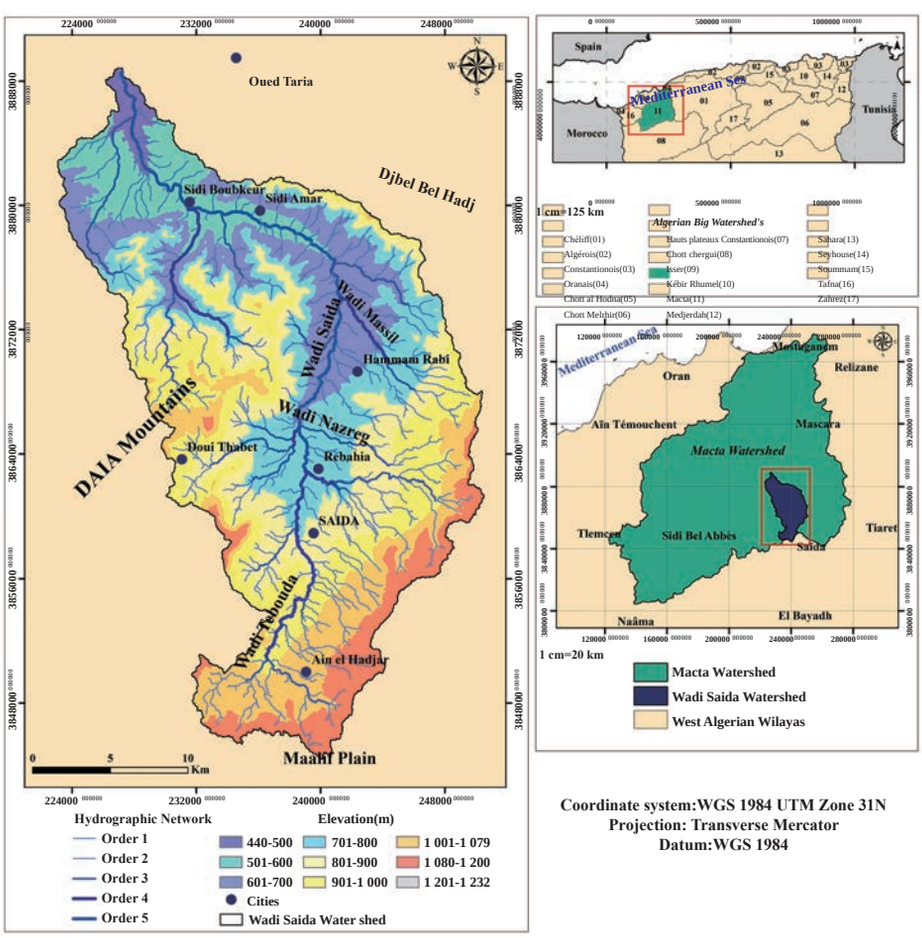

Fig. 1 Location map of the study area (Kessar *et al*. 2020)

2 Materials and method

2.1 Thematic map generation

In this study, six components were used to generate the groundwater potential zone map (geology, slope, lineament density, drainage density, land use and rainfall). The methodology is presented in the following flowchart (Fig. 2). For the Geology map, we have used a digitized map extracted from the 1/200 000 geological map of National Agency of Hydraulic Resources (NAHR, 2008). The lineament density map represents the total length of all recorded and inferred lineaments divided by the surface area under study (Edet *et al*. 1998). An extraction and analysis process is required to determine the linear network before producing the density map. The lineaments network delineated in this study is captured from Landsat 8 (OLI), The Operational Land Imager / (TIRS), Thermal Infrared Sensor image (LC81970362018264LGN00) and SRTM Global 1 arc-second (The Shuttle Radar Topography Mission (SRTM) Collection User Guide, 2015; Shuttle Radar Topography Global Mission 1arc second V003; https://earthexplorer.usgs.gov/), processed by image enhancement and directional filtering (Fig. 4 and Fig. 5). The lithological and structural discontinuities corresponding to structural lineaments were captured on screen by visual analysis. This methodology allowed us to extract lineaments from the study area (Kanohin *et al*. 2012). To interpret and validate the structural lineaments map, we have used the 1/200 000 geological map of the National Agency of Hydraulic Resources (NAHR, 2008) and the 1/50 000 geological map of the NAGMC (National Agency for Geology and Mining Control) (Saprikhine and Riabenko, 1978). After these steps, the lineament density map was produced using the following equation:

$$Ld = \sum_{i=1}^{n} \frac{l_i}{A} \quad (1)$$

Where: l_i is the total lineament length (km) and A is the area of the grid (km^2). The density was classified into different intervals (Table 4). For the highest lineament density interval, the highest-ranking was designated (Pankaj and Amit, 2006). Depending on the understanding of its capacity to promote the occurrence of groundwater, a rank from 1 to 5 is allowed to each lineament buffer zone (Rilo *et al*. 2019).

Streams in the study area are regarded as linear features and displayed as drainage pattern (Adiat *et al*. 2012). To convert the drainage pattern to measurable quantity, Drainage density (Dd) was derived from the drainage pattern by adopting steps similar to those described by Grennbaum(1985).

$$Dd = \sum_{i=1}^{n} \frac{Di}{\mathrm{A}} \quad (2)$$

Where: D_i is the total stream length (km) and A is the area of the grid (km^2). A low infiltration rate is usually due to high runoff with high drainage density of the area, whereas, an area with low drainage density thus represents low runoff and high infiltration (Prasad *et al*. 2008).

For the rainfall map, the yearly average rainfall of 38 years on five stations from the National Agency of Hydraulic Resources was used (NAHR, 2014); rainfall map was then created using inverse distance weight (IDW) interpolation, (Leroux R, 2007), which is widely used by earth scientists (Barier and Keller, 1996) and is one of the most commonly used functions in the spatial data interpolation (Hanquiez *et al*. 2014). This interpolation method is particularly suitable for variable and scattered data such as data from geological surveys or environmental measurements (Huisman and Rolf, 2009). The method is based on the assumption that the rate of correlation and similarity between neighbouring points is proportional to the distance between them, which can be defined as an inverse function of the distance of each point to neighbouring points. Regarding the factors considered important in this method, the neighbouring radius and the power associated with the inverse distance function can be included in the following equation:

$$\mathrm{Zo} = \frac{\sum_{i=1}^{N} Z_i d_i^{-n}}{\sum_{i=1}^{N} d_i^{-n}} \quad (3)$$

Where: Z_0 is the estimated value of variable Z at point i, Z_i is the sample value at point i, d_i is the distance between the sample point and the estimated point, n is the coefficient that determines weight based on distance and N is the total number of predictions for each validation case. From 30 m resolution SRTM GL1 (Shuttle Radar Topography Global Mission 1arc second V003), the slope map was generated using the spatial analyst tool in

ArcGIS 10.4 software.

Finally, the land use types of the basin were derived from the map generated by the National Institute of Soils, Irrigation and Drainage (NISID, 2009). All of these thematic layers are converted to raster file with the same spatial resolution of (30 m) and integrated into ArcGIS 10.4 software to identify groundwater potential zones.

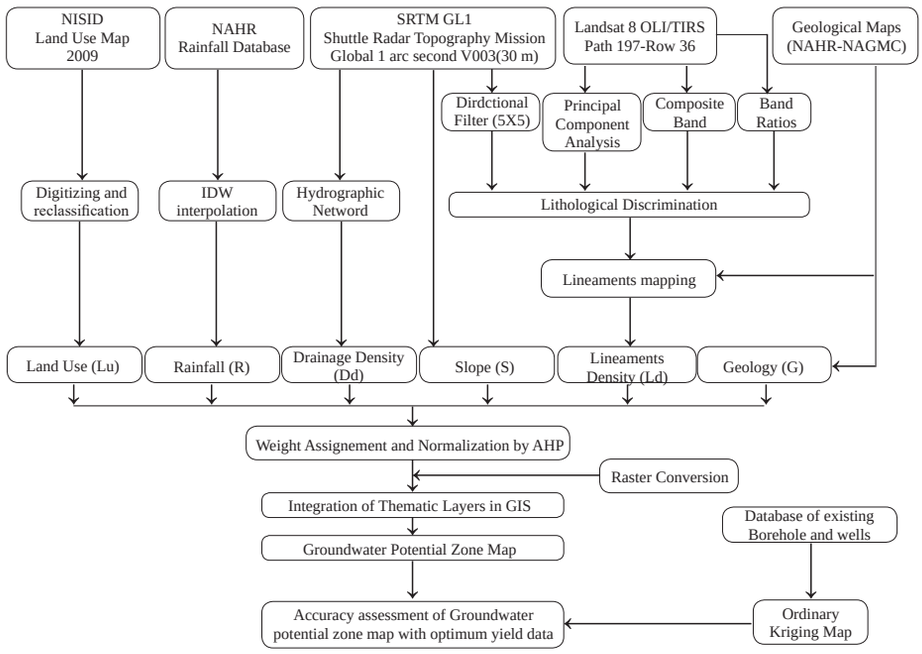

Fig. 2 Flowchart of methodology adopted for delineation of groundwater potential zones

2.2 Assignment and normalization of weights

Analytical Hierarchy Process (AHP) is an organized strategy utilized to investigate complex problems, where an extensive number of interrelated targets or criteria are included (Saaty, 1980). According to the field experience and expert evaluation, the weights are assigned and normalized for different thematic maps using Saaty AHP concept (Saaty, 1980). The subjectivity associated with the assigned weight to different thematic maps as well as their characteristics decreases with the standardization process. Saaty (1980) suggested the calculation of consistency ratio (CR) using the following steps;

Step 1: Principal eigenvalue (λ), is computed by the eigenvector technique.

Step 2: Consistency Index (CI), is calculated from the following equation (Saaty, 1980):

$$CI = \frac{\lambda_{max} - f}{f - 1} \quad (4)$$

Where: f is the number of criteria or factors.

Step 3: Finally, consistency ratio (CR), is calculated as (Saaty, 1980):

$$CR = \frac{CI}{RI} \quad (5)$$

Where: *RI* is the random indexes whose values depend on the order of the matrix. In our case, a matrix of 6 factors or criteria are used and the RI values are adopted from Alonso and Lamata (2006) (Table 1). The value of RI was obtained from the Saaty scale from 1 to 9. The value of CR should be less than 10% (Prasad *et al*. 2008) for consistent weights. After calculation using an AHP Excel template with multiple inputs and five decision-makers analysis (Klaus, 2013), the consistency ratio CR was 3.3%, then the relative weights can be re-evaluated to prevent confusion (Shekhar and Pandey, 2014). A denotative 9-point scale was used for the prioritization operation and to generate the pair-wise comparison matrix, where 1, 3, 5, 7 and 9 represent important, moderately important, strongly important, very strongly important and extremely important (Table 2). The intermediate values 2, 4, 6 and 8 could be used when compromise is needed (Gdoura *et al*. 2015). For each previous layer a new rate is given to each category class and this rate indicates the ranges of groundwater potential associated with each factor.

Rates were assigned to each class according to the order of the influence of the class on groundwater potential (Table 4), ratings of 1 to 5 were adopted, representing very low, low, medium, high and very high groundwater potential (Kumar *et al*. 2014).

Table 1 Random indices for matrices of various sizes (Alonso and Lamata, 2006)

N	3	4	5	6	7	8	9	10	11	12
RI	0.524 5	0.881 5	1.108 6	1.247 9	1.341 7	1.405 6	1.449 9	1.485 4	1.514 1	1.536 5

Table 2 Calculation of effects and rates of factors affecting groundwater potentiality (Saaty, 1980)

Option	Numerical value (s)
Equal	1
Strong	3
Strong	5
Very strong	7
Extremly strong	9
Intermediate values	2, 4, 6, 8
Reflecting dominance of second alternative compared with the first	Reciprocals

2.3 Delineation of groundwater potential zones

For the delineation of the groundwater potential zones, the groundwater potential index (GWPI) was used. Thematic maps from various sources were collected, including remote sensing and conventional data. All the themes and features of the study area were considered and integrated (Kessar *et al*. 2020). To estimate the groundwater potential index (GWPI) (Rao and Briz-Kishore, 1991; Malczewski, 1999; Shekhar and Pandey, 2014; Rahmati *et al*. 2015; Maity and Mandal, 2017; Nithyaa *et al*. 2019), a weighted linear combination method was used as follows:

$$GWPI = \sum_{w=1}^{m} \sum_{i=1}^{n} (W_i X_j) \quad (6)$$

Where: W_i represents the normalized weight of the *i*-th thematic layer, X_j is the rank value of each class of the *j* layer, *m* is the total number of thematic layers, and *n* is the sum number of classes in the thematic layer. In this study, GWPI is calculated as:

$$GWPI=Ld_wLd_r+G_wG_r+Dd_wDd_r+R_wR_r+S_w\,S_r+Lu_wLu_r \quad (7)$$

Where: Ld_w is the weight of lineament density and Ld_r represents its attributed rank; Dd_w is the weight of drainage density and D_d represents its attributed rank; S_w is the weight of slope and S_r represents its attributed rank; R_w is the weight of rainfall and R_r represents its attributed rank; Lu_w is the weight of land use and Lu_r represents its attributed rank; G_w represents the weight of geology classes and G_r is its attributed rank. The Raster Calculator tool allows us to create and run the map algebra expression of (GWPI) to generate the groundwater potential map. After assigning the rank to the rating classes, each thematic raster is multiplied by the normalized weights and the result is saved as a new raster. The addition of these resulting raster layers will provide us with the final map of groundwater potential zones.

2.4 Validation using geostatistic analysis

Geostatistics is a branch of statistics which studies the spatial connections of datasets and variables in order to discover and analyze any quantifiable phenomenon. Geostatistical study is based on the theory of spatial or spatiotemporal variables, and its primary objective is to highlight, when it exists, the spatial structuring of the phenomenon and to estimate or predict this phenomenon. The mathematical tool of geostatistics is the experimental variogram or semivariogram (Koudou *et al*. 2014). Kriging is one of the geostatistical techniques for spatial modelling, which takes spatially dispersed data as input

to obtain a generalized representation of this information (Hennequi, 2010). Kriging refers to the semivariogram, which is calculated using the following formula:

$$\gamma(h) = \frac{1}{2N(h)} \sum_{i=1}^{N(h)} (Z(x_i + h) - Z(x_i))^2 \quad (8)$$

Where: $Z_{(xi)}$ is the value of the variable Z at location of $N(h)$, h is the lag, and $N(h)$ is the number of pairs of sample points separated by h. For random sampling, it has little chance that the distance between the sample pairs to be exactly h, wherefore h is usually represented as a distance range. Calculating the semivariogram values at several lags can help produce a semivariogram plot. These values are then fitted with a theoretical model: Spherical, exponential, or Gaussian. These models provide information on the input parameters for the Kriging interpolation as well as on the spatial structure of variables. Kriging is a type of weighted moving average method, which is also an optimal spatial interpolation method (Nas, 2009):

$$\hat{Z}_{(x0)} = \sum_{i=1}^{m} W_i Z_{(xi)} \quad (9)$$

Where: $\hat{Z}_{(x0)}$ is the value to be estimated at the location of x_0; $Z_{(xi)}$ is the known value at sampling site x_i, and W_i is the weight. In the present study, among the different kriging techniques, the ordinary kriging (OK) method was used due to its simplicity and its prediction accuracy compared to other kriging methods (Isaaks and Srivastava, 1989). To carry out the geostatistical modelling, data from 47 existing and operating boreholes including their operating yield (pumping rates) from the National Agency for Hydraulic Resources (2018) were used to produce the spatial distribution map of borehole yields by ordinary kriging. Among these borehole, 22 are distributed in the watershed and others in the peripheral areas.

3 Results

3.1 Factors influencing groundwater potential

3.1.1 Geology (G)

Groundwater potential is significantly dominated by lithology (Das and Pal, 2019). According to Fig. 3, four geological classes are identified in the study area based on their respective importance and effect on groundwater potential. The major geological types are Alluvium, Sandstone, Limestone and Granites. Alluviums play a significant role in groundwater supply than other geological formations. They are characterized by good permeability. In the study area, alluvium is widely distributed in the wadi Saida valley, which represents the rainwater collection area. The surface drainage network promotes the accumulation of surface flows in this area. Limestones are well exposed in the extreme northern part of Sidi Boubkeur and Sidi Amar and also the southern part of the watershed in Ain al Hadjar. Sandstone formation covers both the eastern and western part of the wadi of Saida. These formations are moderately favourable for groundwater recharge. The granite formations situated in the north of Hammam Rabi generally have very low groundwater potential except where they are fractured.

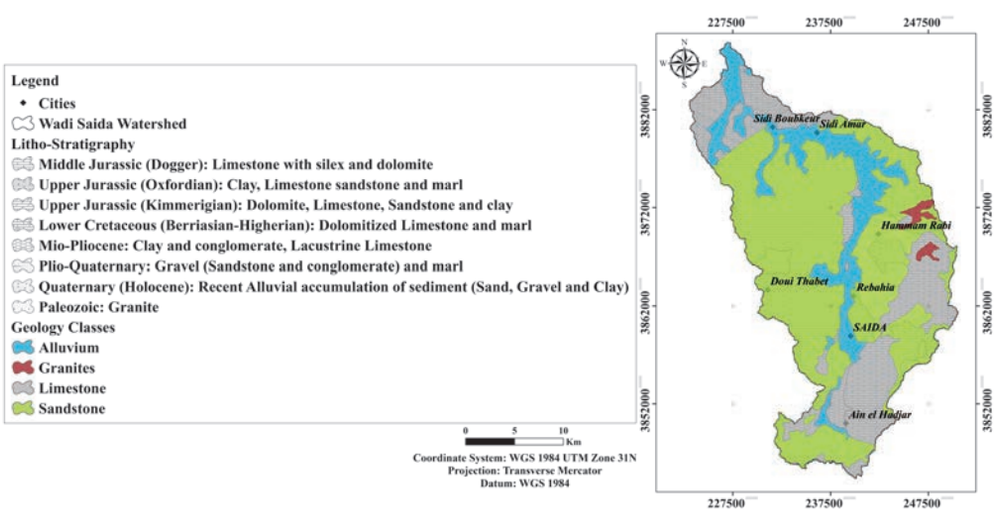

Fig. 3 Geological map of Wadi Saida Watershed (After NAHR, 2008)

The study area is marked by the presence of two water tables, a shallow water table and a karst water table. The first one is located exclusively in the valley of the wadi Saida and in the upper layers of the Saida formation and the plio-quaternary deposits (clay sands, calcareous clays and conglomerates). The karstic aquifer is situated in the carbonate sediments of the Lower and Middle Jurassic with a captive part in the valley and a free part in the rest of the aquifer (mainly Nador carbonate formation).

3.1.2 Lineament density (Ld)

Lineaments are linear features of tectonic origin that are long, narrow and relatively straight alignments. They are visible on satellite images as tonal differences compared to other terrain features (Klaus, 2013). The distinguished lineaments may be the result of fracturing or fault system which indicates the possibility of increased porosity and permeability zone in hard rock and is consequently of importance in groundwater studies (Adiat *et al*. 2012).

Lineament extractions-the maps of the lineaments network in this study are interpreted from Landsat 8 OLI/TIRS through image processing, such as lithological discrimination by the processing of composite band, band ratios, and principal component analysis (Fig. 4). Directional filtering of the SRTM GL1 (Shuttle Radar Topography Global Mission 1arc second V003) was also used (Fig. 5). Lineaments derived only from natural topographical features are indicators of groundwater flow-paths, therefore their hydrogeological importance needs to be evaluated (Jordan *et al*. 2005; Sander, 2007). The boundary contacts of two or more geological formations are also important in identifying high groundwater potential zones. The validation process consists of removing anthropic activities to leave only the contours and lines effectively corresponding to the lineaments (Koita *et al*. 2010), and observing the fracturing network already existing or assumed in the geological maps and the lineaments of geological contact or lithological and structural discontinuities. The application of the directional filter (5×5) allowed the mapping of 77 lineaments in Wadi Saida Watershed concentrated in the southern part of the basin in close proximity of the city of Saida. The filtering was carried out in different directions, *i.e*. 0°, 45°, 9°, 135°, 180°, 225°, 270°, 315°, only the directions of 45°, 90°, 135° and 225° are identified and merged (Fig. 5).

Statistical Analysis of lineament was performed by the development of two-directional rosettes; the first represents the percentage of lineaments regarding the total length, and the second indicates the number of lineaments to the total number (Fig. 6 and Fig. 7). The statistical analysis of lineaments has been explored by several authors to study the geometry of the lineament network and to identify the dominant directions at the regional scale (Pretorius and Partridge, 1974).

The conventional method consists of producing directional rosettes against the cumulative length of the lineaments in classes of 10° of orientation. The two directional rosettes show a nearly even distribution of percentage of the lineaments in both total length and total number of lineaments. The results show that 49.35% of the lineaments' directions are in the range of 10°~70° whereas 10.39% of them are SW-NE within the range of 60°~70°) which is the most dominant direction. Regarding the length of the lineaments, the ones with the SW-NE direction are also dominant, and 21% of the total length of the lineaments have the direction between 40° and 80°.

The statistical analysis of the lineament network shows that this direction is secondary because it represents only 18% of the total number of lineaments and 28% of the total length. The lineament density of the watershed varies from 0 to 2.5 km/km^2 (Fig. 8) and was reclassified into five classes, *i.e*. <0.5 km/km^2, 0.5~1 km/km^2, 1~1.5 km/km^2, 1.5~2 km/km^2 and >2 km/km^2, where the first two classes represent 85% of the basin area (Fig. 8). The comparison between the lineaments' direction and the piezometric analysis by Dahmani (2016) shows that the underground flow direction and that of the lineaments are identical, implying strong possibility of recharge of karstic aquifer by water percolated through the faults network.

3.1.3 Rainfall (R)

Rainfall is one of the main sources of groundwater recharge. More rainfall in any given region indicates higher groundwater potential recharge (Machiwal *et al*. 2011). Intensity and duration of

rainfall significantly affect groundwater recharge and potential (Wondifraw *et al*. 2019). In the Wadi Saida Basin the annual average rainfall ranges from 300 mm to 330 mm, and the southern part of the basin receives higher precipitation but is of stormy character (Fig. 9).

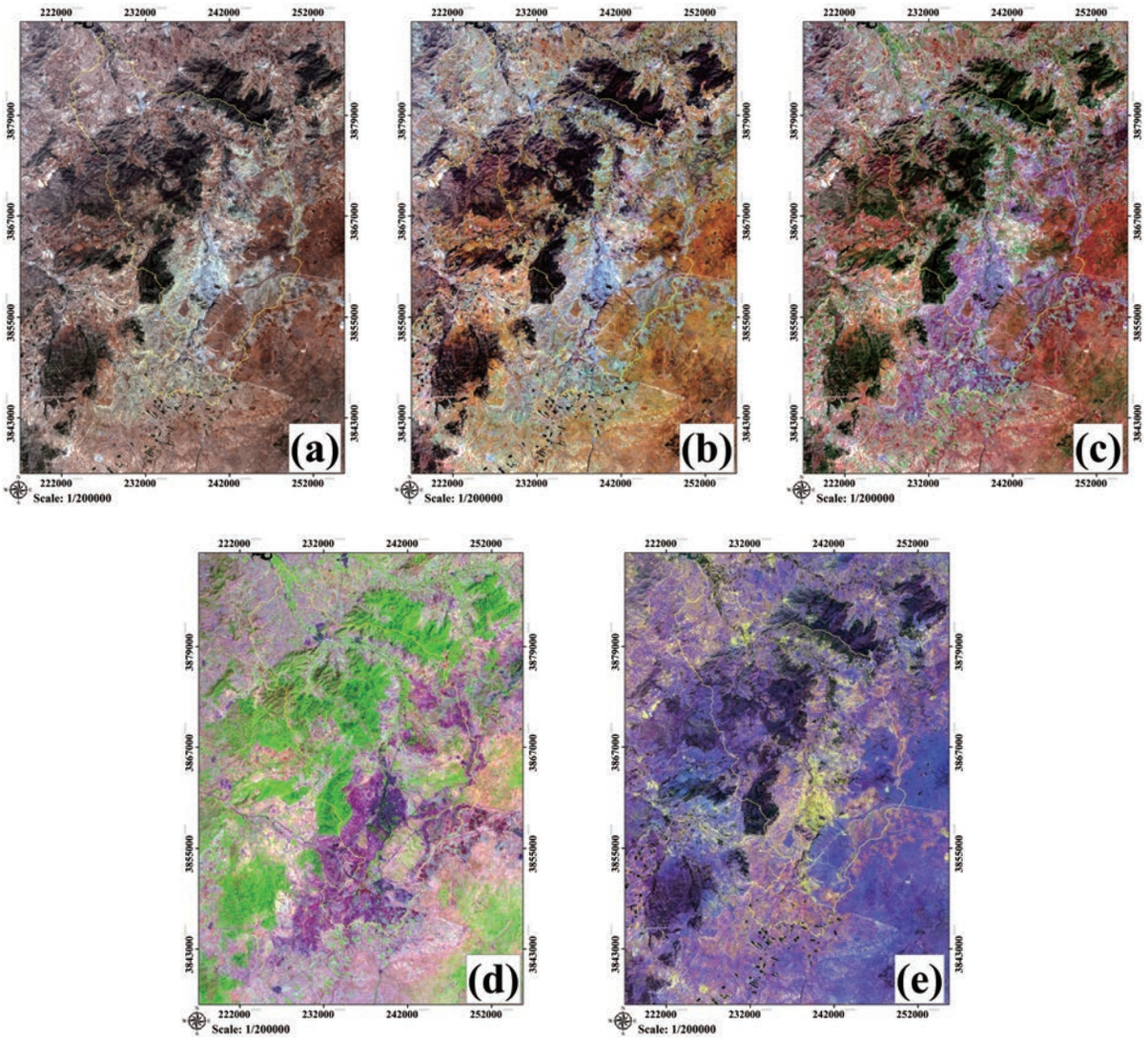

Fig. 4 Different lithological discrimination process applied to the Landsat 8 image: (a) RGB (432), (b) RGB (742), (c) RGB (753), (d) Band ratios (6/2, 5/3, 4/2), (e) PCA (PC1, PC2, PC3)

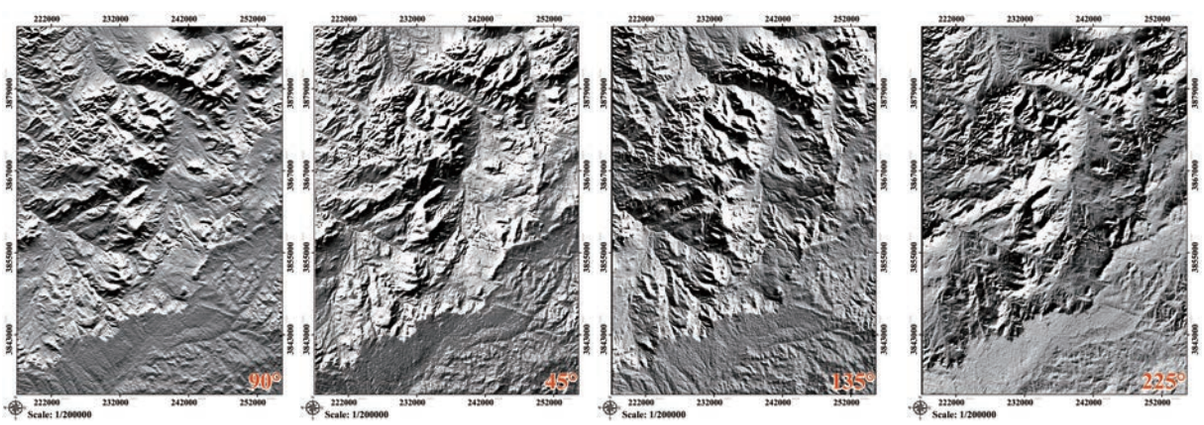

Fig. 5 Directional filtering applied to the SRTM image (45°, 90°, 135° and 225°)

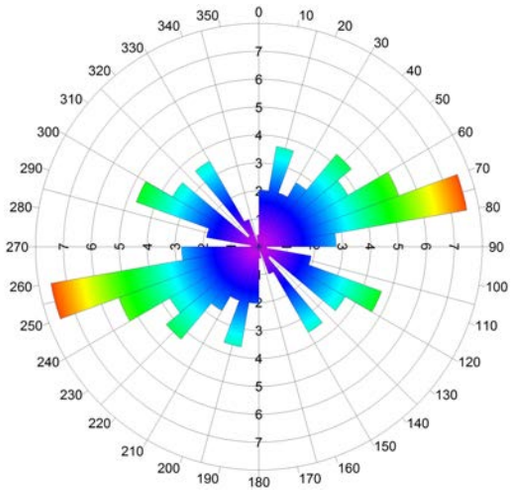

Fig. 6 Directional rosette of lineaments as percent of total number of lineaments

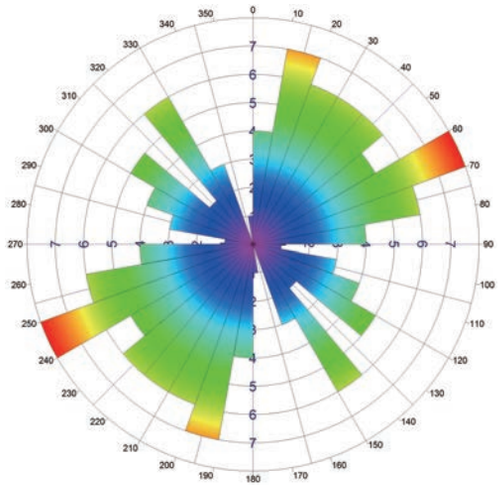

Fig. 7 Directional rosette of lineaments length as percent of total lineament length

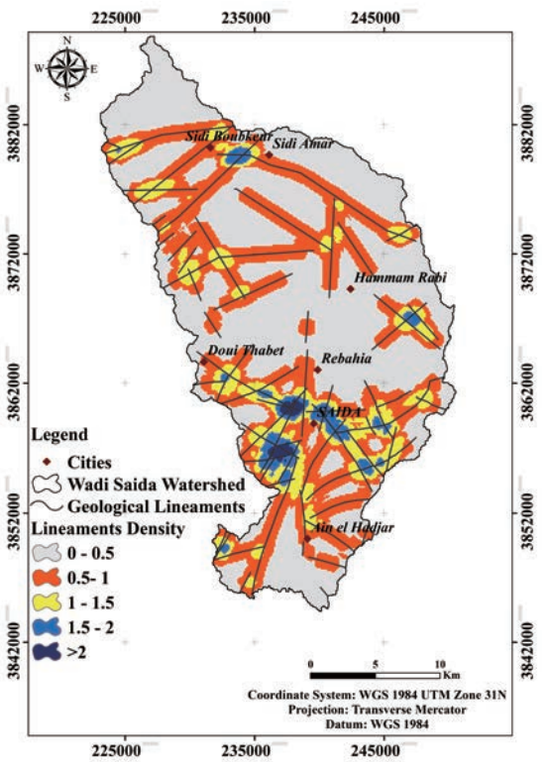

Fig. 8 Lineament density map

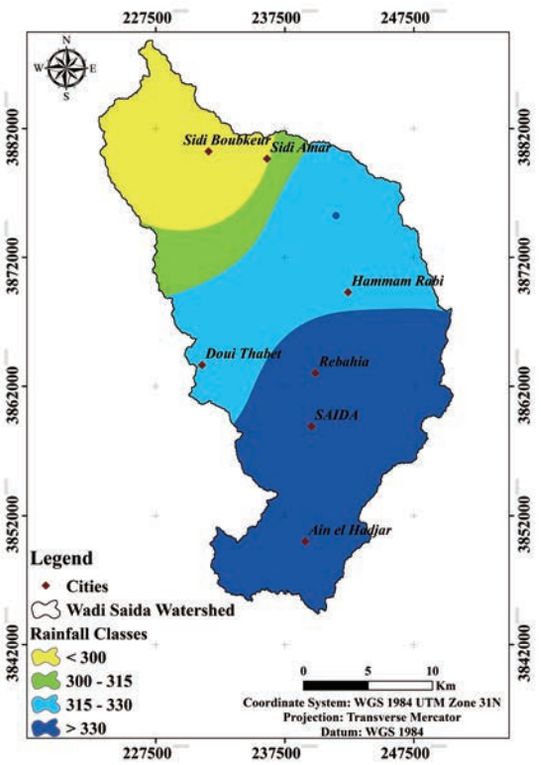

Fig. 9 Rainfall map

3.1.4 Slope (S)

Slope is presented as a degree, indicating the capacity of surface water to flow and reach the groundwater reservoir. This factor is extremely necessary for the identification of favourable groundwater recharge sites, as it directly affects run-off intensity, surface water infiltration and recharge (Nouayti *et al*. 2017). Slope is an indicator for the suitable groundwater prospect (Klaus, 2013).

The high degree of slope results in a rapid downward flow of surface water and a short infiltration time, indicating a low recharge level. However, the low degree of slope tends to increase recharge because of the increased retention of rainwater (Nouayti *et al*. 2019). The slope of the Wadi Saida Watershed was divided into five classes: <3°, slight slope (3°~7°), moderate slope (7°~12.5°), steep slope (12.5°~25°), and very steep slope (>25°) (Fig. 10). The areas with steeper slope cause relatively high run-off and

low infiltration, and hence are categorized as poor and have less groundwater accumulation (Jha *et al*. 2010).

3.1.5 Drainage density (Dd)

The drainage density of the Waidi Saida Watershed ranges between 2.22 km/km^2 and 3.33 km/km^2 (Fig. 11), which was reclassified into three classes, viz, low (<2.5 km/km^2), moderate (2.5~3 km/km^2), and high (>3 km/km^2). 52% of the study area falls in the moderate class of drainage density, followed by low (36.4%) and high drainage density class (11.6%) (Fig. 11).

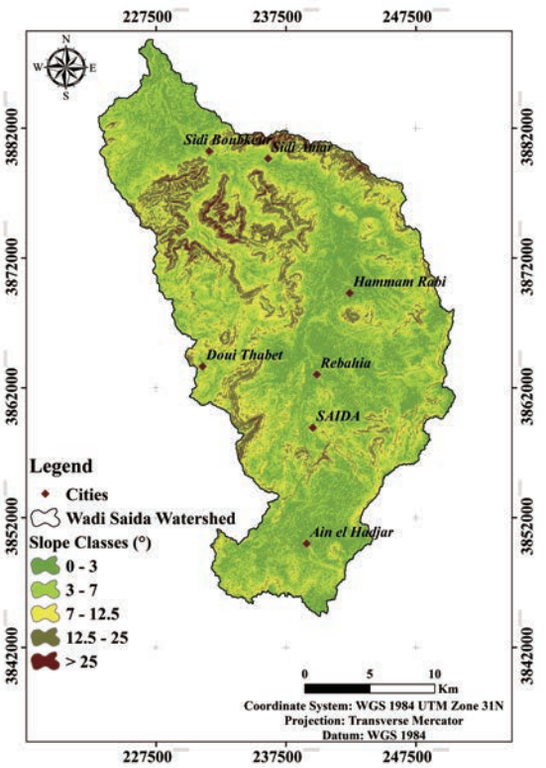

Fig. 10 Slope map

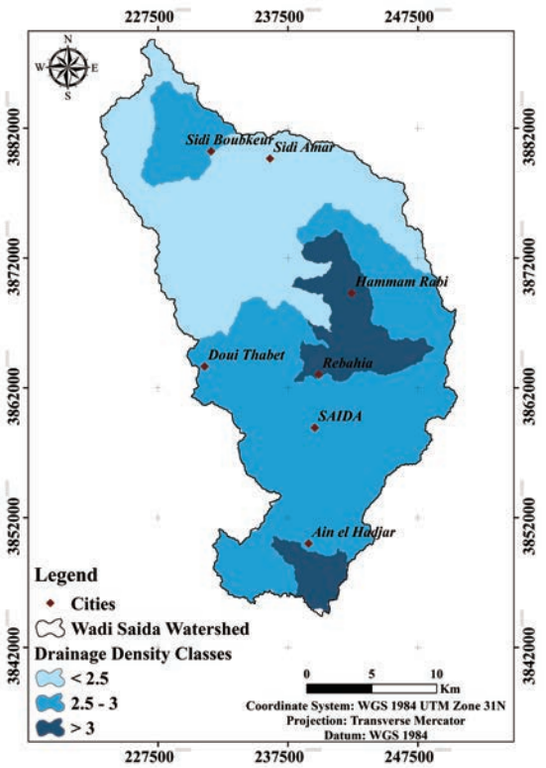

Fig. 11 Drainage density map

3.1.6 Land use (Lu)

Land use map was generated by the National Institute of Soils, Irrigation and Drainage (NISID, 2009) to reclassify and rank the new land use categories of the study area (Fig. 12). The new groups were reclassified as follows: Forest class, including dense maquis, dense forest and clear forest; built class, including agglomeration, airport and built-up; and shrubland class, including brush and clear maquis, and Agriculture and barren soil class, which remained the same.

3.2 Groundwater potential zones

The application of AHP techniques on the weighted components has allowed the mapping of groundwater potential zones in raster format in ArcGIS. In the pair-wise comparison matrix

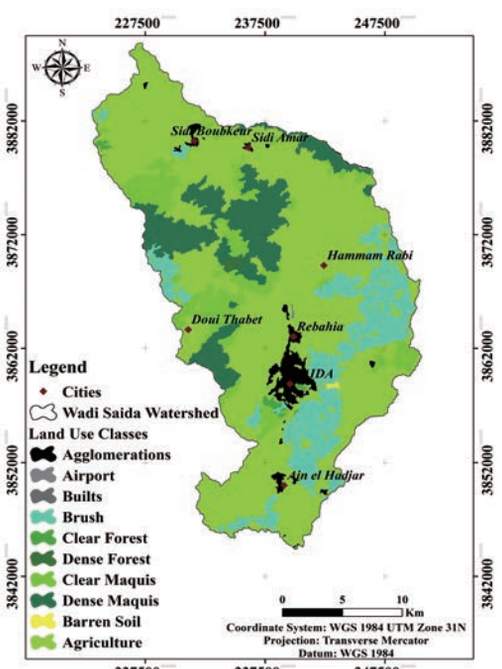

Fig. 12 Land use map

(Table 3), factors of influence are reciprocals of each other and a normalized weight estimated in percent is given.

The calculation of the normalized weight of the layers revealed that lineament density had the greatest weight (44.8%), which is justified by the fact that the zone is characterized by the presence of a karstic aquifer where fracturing plays an important role in groundwater recharge. Precipitation is also an important factor and a weight of 20.44% is applied.

The weight of the geology factor is 14.47% and it shows that the alluvial and limestone-dolomitic zones have the highest rating (Table 4). The final groundwater potential map of the Wadi Saida Watershed using the AHP method shows four areas (Fig. 13), *i.e*. 32.39% of the total area, or 202 km^2, is classified as good and very good groundwater potential zone; 65.76% of the area is classified as moderately potential zone and only 1.85% as the low potential zone (Table 5).

Table 3 Pairwise comparison matrix and percent normalized weights of used criteria

Matrix	Dd	G	Lu	R	S	Ld
Dd	1	0.53	1	0.33	0.68	0.15
G	1.9	1	3.88	0.72	1.9	0.21
Lu	1	0.26	1	0.34	0.78	0.16
R	3	1.38	2.91	1	2.04	0.72
S	1.48	0.53	1.28	0.49	1	0.16
Ld	6.88	4.83	6.35	1.38	6.35	1

Table 4 Classification of influencing factors for groundwater potential zones

Influencing factors	Category class	Rank	Rating	Normalized weight (%)
Lineament density (km/km^2)	>2	5	Very good	44.80
	1.5~2	4	Good	
	1~1.5	3	Moderate	
	0.5~1	2	Poor	
	0~0.5	1	Very poor	
Geology	Alluvium	5	Very good	14.47
	Limestone	4	Good	
	Sandstone	3	Moderate	
	Granites	1	Very poor	
Rainfall (mm)	>330	5	Very good	20.44
	315~330	4	Good	
	300~315	3	Moderate	
	<300	2	Poor	
Slope (°)	0~3	5	Very good	8.09
	3~7	4	Good	
	7~12.5	3	Moderate	
	12.5~25	2	Poor	
	>25	1	Very poor	
Drainage density (km/km^2)	>3	5	Very good	6.29
	2.5~3	4	Good	
	<2.5	3	Moderate	
Land use	Forest	5	Very good	5.91
	Schrub land	4	Good	
	Agriculture	3	Moderate	
	Barren land	2	Poor	
	Built up	1	Very poor	

Table 5 Area statistics of groundwater potential zones

S.N	GWP class	Area (km^2)	Percentage from total area
1	Poor	11.56	1.85
2	Moderate	410.77	65.76
3	Good	188.21	30.13
4	Very Good	14.12	2.26

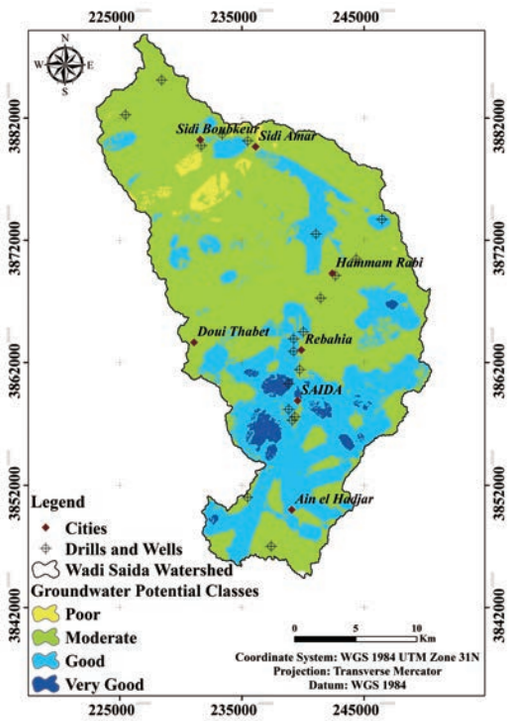

Fig. 13 Groundwater potential map using AHP model of Wadi Saida Watershed

3.3 Accuracy assessment and validation

Geostatistic approach was used to validate the groundwater potential map. It involves questions about how data in different layers can relate to each other, and how it varies in space (Huisman and Rolf, 2009).

In the present work, we applied the ordinary kriging method, of which the stationary variable of the mean is unknown and the variogram $\gamma(h)$ reaches a plateau where it grows less rapidly than h^2. The nugget effect represents the abrupt variation of the measured parameter (Table 6) (Fig. 14). The correlation clouds compare the measured values (in abscissas) against the estimated values (in ordinates), and a good correlation coefficient of 0.87 has been achieved (Table 7). According to the model obtained from the estimation error (Fig. 15), the adjusted ordinary kriging is more accurate because the average error is closer to zero and the standard deviation of the estimation errors is small (about 41%).

Table 6 Model characteristics

Parameter	Valor
Nugget effect	492.05
Type	Gaussian
Major range	4 506.48
Sill	1 293.48
Lag size	626.73
Number of lags	12

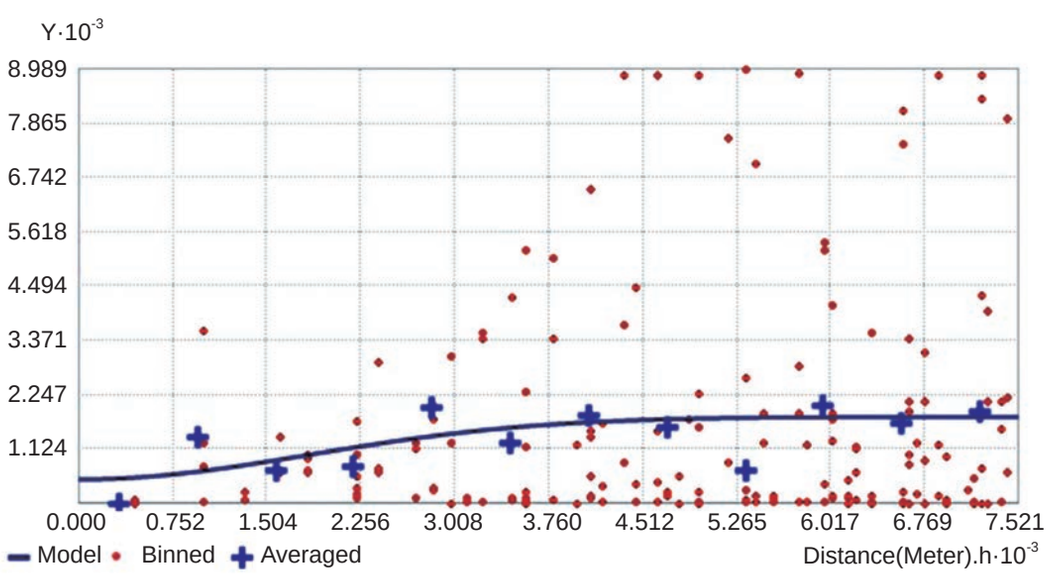

Fig. 14 Semi-Variogram of estimated flows

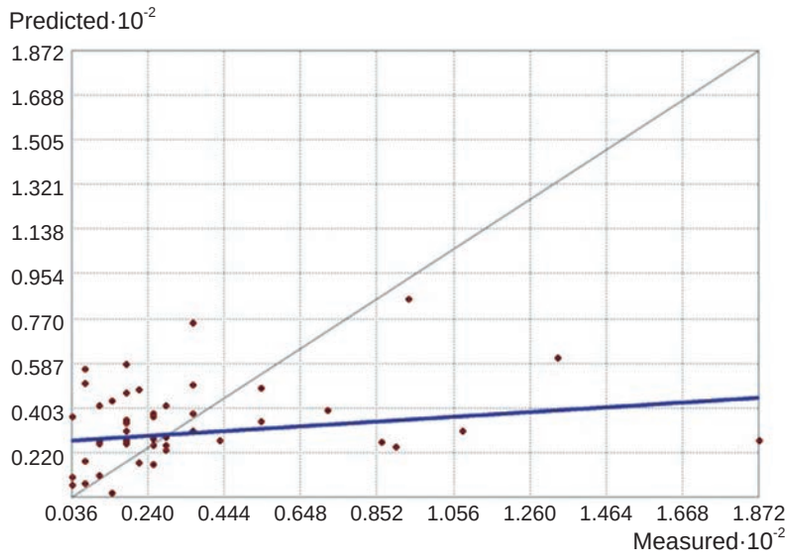

Fig. 15 Regression of the measured values according to the estimated values

Table 7 Correlation function characteristics

Function	0.096X+26.60
Samples	47 of 47
R^2	0.87
Standard average error	40.97

The spatial distribution of borehole yield was generated using ordinary kriging on a set of 47 boreholes with yield data. Three zones were identified to fill the areas which were not delineated before we added neighbourhood boreholes to the watershed (Fig. 12). The borehole yield is classified into four class: Poor (0 m^3/h to 10 m^3/h), moderate (10 m^3/h to 50 m^3/h), good (50 m^3/h to 75 m^3/h) and very good (>75 m^3/h) (Fig. 16). An accuracy assessment to validate the results was performed by comparing the actual yield of 21 boreholes in the field and the estimated optimum yield from the two maps produced (Ordinary Kriging map of existing borehole yield and the GWP map) (Fig. 13 and Fig. 16).

The procedure can be described as follows, if the classification results are the same or similar from the three sources of input (actual yield from the field, estimated yield from the kriging map and estimated yield from the GWP map), we may conclude that an agreement status has been reached between the estimated and the actual yield. On the other hand, if these classes are different, we may state that there is a disagreement between the estimated and actual yield. A partial agreement can be presented when close values are found between two sources of inputs of the three (Table 8). Out of the 21 wells, optimum yield of 15 wells, or 71% of the total number of wells, suggests that there is a partial or full agreement between the estimated yield using Kriging map (Fig. 16) or Groundwater potential map (Fig. 13) and the actual yield of boreholes. The rest 6 boreholes show an absolute disagreement between the estimated and actual yield.

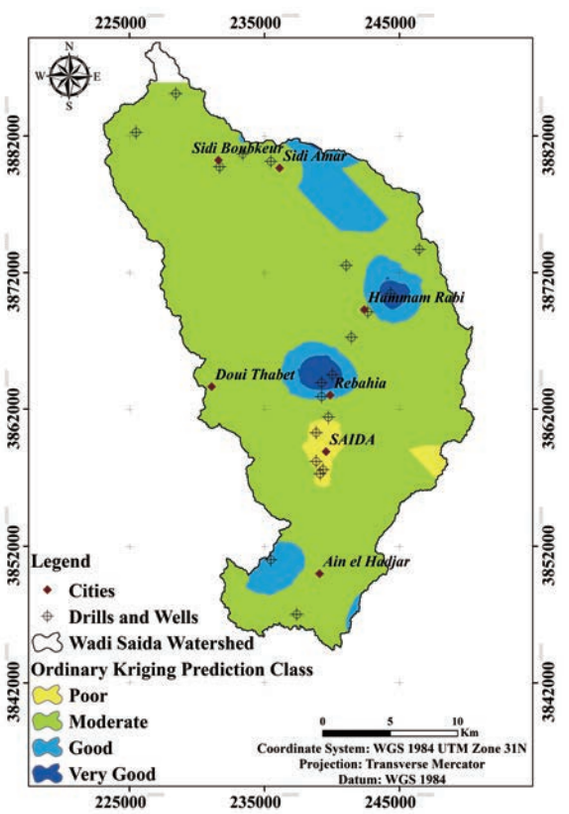

Fig. 16 Ordinary Kriging map of existing borehole yield

Table 8 Accuracy assessment of groundwater potential zone map with optimum yield data

Well N°	Actual yield (m^3/h)	Actural yield class	Estimated yield (m^3/h)	Estimated yield class (Kriging map)	Estimated yield class (GWP map)	Agreement estimated-actual yields description
01	21.6	Moderate	28.0	Moderate	Moderate	Agree
02	86.4	Very good	68.8	Good	Moderate	Partially agree
03	3.6	Poor	5.8	Poor	Very good	Disagree
04	3.6	Poor	9.0	Poor	Moderate	Disagree
05	36.0	Moderate	57.5	Good	Good	Agree
06	7.2	Poor	12.3	Poor	Moderate	Disagree
07	14.4	Poor	8.9	Poor	Good	Disagree
08	7.2	Poor	8.7	Poor	Moderate	Disagree
09	7.2	Poor	18.8	Moderate	Good	Disagree
10	93.6	Very good	89.3	Very good	Good	Partially agree
11	133.2	Very good	90.0	Very good	Good	Partially agree
12	10.8	Poor	20.8	Moderate	Moderate	Agree
13	36.0	Moderate	41.2	Moderate	Moderate	Agree
14	108.0	Very good	84.1	Very good	Moderate	Agree
15	25.2	Moderate	28.4	Moderate	Good	Agree
16	18.0	Moderate	31.7	Moderate	Moderate	Agree
17	18.0	Moderate	21.6	Moderate	Moderate	Agree
18	54.0	Good	46.3	Moderate	Moderate	Agree
19	28.8	Moderate	28.0	Moderate	Moderate	Agree
20	36.0	Moderate	36.8	Moderate	Moderate	Agree
21	36.0	Moderate	36.8	Moderate	Moderate	Agree

4 Discussion

The Wadi Saida Watershed is recognized as the major target for groundwater exploitation since it is the main source of water supply in the region. Boreholes are generally deep (more than 150 m) with yields ranging from several m^3/h up to more than 100 m^3/h. The application of Analytical hierarchy process (AHP) method has shown that some criteria have more influence than others. In this study, the lineament density carries the highest weight, followed by geology. Rainfall in the study area is characterized by irregular and intense events in the autumn, which disturbs the groundwater recharge and causes high groundwater demand in irrigation and other activities. The slope also plays an important role where runoff and infiltration have the great impact on groundwater recharge.

According to the directional filtering of lineaments, the dominant direction is the SW-NE, in which the latter is due to the alpine orogeny. This type of tectonics affects the ancient formations characterized by large folds giving rise to the Saida Mountains. A dense lineament network is present where the most important lineaments are located along the border of the Saida city towards the northwest (faults of Zeboudj) and the southeast. In the southeastern part of the watershed, a geological contact between the karst aquifer system and other aquifers is located. Multiple faults are presented in this area allowing the discharge of water to the deepest aquifer in contact. Those aquifers in the Rebahia zone can provide a good supply of groundwater.

According to Bencherki (2008), the structures of the Viseean orogeny are corresponding to faults and folds with the directions of NE and NE-SW. The uplift also caused the deformation of the Jurassic dolomitic cover, while a collapse ditch along N-S axis was developed in the Saida valley. These differentiated uplift movements have generated brittle tectonics in the region. The

principal directions are approximately SW-NE to NNE-SSW. Tectonic events are mostly sub-vertical (Bencherki, 2008).

The karstic aquifer extends over the Saida Mountains, part of which is located on the south-eastern side of the watershed and the other part is outside the basin. A vertical impermeable flow boundary presents in the southwest generated by two perpendicular faults to the west. These faults form an impermeable substratum which limits the water table to its northwest. Thus, it is bordered by a discharge line along the Triasopaleozoic basement aquifer and the edge of the Ain Soltane and Ain Balloul plateaus, and an impermeable contour in the Djebel Mozdbab area with a cut in the aquifer in the north sector of Mozdbab horst. To the northeast, the diagonal fault of the eastern flank of the Tiffrit mole is an impermeable boundary. According to Djidi *et al*. (2008), the saida valley is devoided of epikarst as evidenced by the intensely fractured outcrops as well as the presence of caves and chasms with several meters in diameter (Boukhors, Ain Zerga, Vieux Saida, Bir H'mam). The karstic system can be divided into two formations: One is in the surface mainly occurred in Tidernatine plateau as sinkholes, losses and backslides giving rise to funnels like Ghar Ouled Amira, Ghar Slouguia; the other one is at the bottom where sinkholes may evolve with collapse of the underlying karstic void (Bir H'mam well) and other deep ones whose system is drained by the source of Ain Zerga, the underground river of Bir H'mam and the loss of Ghar Ouled Amira. This river could be the principal collector of the karstic system of Tidernatine. The losses could feed the underground river of Bir H'mam and the resurgence of Ain Zerga.

Previous studies (Pitaud, 1973 in Dahmani, 2016 and Djidi *et al*. 2008) have shown that the series of Jurassic carbonates resting on the impermeable substratum of Triassic clays form the main aquifer in the region. With local aquifers, Upper Jurassic and Lower Cretaceous sandstones can be drained down towards the underlying carbonate aquifer while the network of existing faults can play the interconnectivity role between these aquifers, which demonstrates the importance of lineament density in the study of the potential of groundwater. Also, as our study has proven, these previous studies showed that the Jurassic carbonate formations are influenced by faults oriented NE-SW especially in the Wadi Saida valley, where the lineament density is higher than other parts of the watershed. The spatial coverage of precipitation around the slope gradient of water points in conjunction with the hydrographic network substantially influences the infiltration rate. Runoff increases and affects negatively the potential groundwater areas (Kumar *et al*. 2014). Land use analysis provides important indicators of the extent of groundwater demands and its usage, as well as an important indicator in the selection of sites with good groundwater potential. Demographic data and new urban areas as well as regions with significant agricultural potential are also needed in the planning of new borehole sinking projects.

From the Groundwater Potential map using AHP model (Fig. 15), areas with high estimated borehole yields are located in the northeast of the Wadi Saida Watershed, west of Ain Soltane and Hammam Rabi and the region of Ain el Hadjar which is characterized by the presence of discontinuous aquifers with cracks and karstic features composed mainly by upper Cretaceous limestones and dolomitized and marl-limestones from the lower Cretaceous. Estimated average flow rates are observed in the West of Sidi Boubkeur and Doui Thabet, characterized by the presence of carbonate sediments from discontinuous aquifers of the upper and middle Jurassic. Low values are concentrated in the city of Saida and the extreme eastern zone of the study area, which represent the boundary between the continuous aquifers of the quarter-century and the discontinuous karst aquifers. While, the Ordinary Kriging map of existing borehole yields (Fig. 16) show also that, the very good to good estimated flow class were located in the north-eastern part of the basin on Sidi Boubkeur region, the area of Hammam Rabi and Rebahia, as well as the south-west part of Ain el Hadjar.

Geostatistical analysis of 47 wells was used in this study to validate of the groundwater potential map produced with the data from existing boreholes. Variographic analysis showed a good correlation between the actual values and those estimated. According to the results, the correlation between the estimation zones (groundwater potential zone map) and the spatial distribution of actual borehole yields (Ordinary Kriging map of

existing borehole yields) is concluded. The results indicate that the southern part of the basin is more favorable for groundwater exploitation, the north of Sidi Boubkeur and Sidi Amar and the south of Ain El Hadjar and the far west of Doui Thabet.

As a result, the mapping of groundwater potential through the Remote Sensing and GIS-based AHP approach could be applied with satisfaction. Consequently, these results can be utilized for better planning and management of groundwater resources, borehole siting, and maintaining the sustainable exploitation of areas.

5 Conclusions

In this study, an integrated approach of GIS-based Analytical Hierarchical Process is used to delineate the groundwater potential zone in Wadi Saida watershed. Six layers were selected as influencing factors (geology, lineament density, rainfall, drainage density, slope and land use). The processing and interpretation of SRTM and Landsat 8 OLI images has provided good results in the mapping of geological lineaments present in the Saida region. Groundwater potential in the study area is mainly controlled by lineament density, geological settings and rainfall, while slope, drainage density and land use are considered as secondary factors. The groundwater potential map using AHP shows that the whole study area can be classified into four groundwater potential zones, such as Very good (2.26% of the area), Good (30.13% of the area), Moderate (65.76% of the area), and Poor (1.85% of the area).

This study confirms the efficiency of using remote sensing and GIS for the identification of groundwater potential zone through AHP techniques and geostatistic analysis in semi-arid regions. The current study provides highly valuable knowledge to decision-makers for planning and framing new strategies for sustainable groundwater development and water resources management.

References

Adiat KAN, Nawawi MNM, Abdullah K. 2012. Assessing the accuracy of GIS-based elementary multi criteria decision analysis as a spatial prediction tool (A case of predicting potential zones of sustainable ground water resources). Journal of Hydrology, 440-441: 75-89.

Alaa AA, Ayser AS. 2015. Groundwater potential mapping of the major aquifer in northeastern missan governorate, South of Iraq by using analytical hierarchy process and GIS. Journal of Environment and Earth Science, 4(10): 125-150.

Alonso JA, Lamata MT. 2006. Consistency in the analytic hierarchy process: A new approach. International Journal of Uncertainty Fuzziness and Knowledge Based Systems, 14(4): 445-459.

Balasubramani K. 2018. Physical resources assessment in a semi-arid watershed: An integrated methodology for sustainable land use planning. ISPRS Journal of Photo-grammetry and Remote Sensing, 142: 358-379.

Bartier PM, Keller CP. 1996. Multivariate interpolation to incorporate thematic surface data using inverse distance weighting (IDW). Computers and Geosciences, 22(7): 795-799.

Bencherki A. 2008. Réalisation d'une carte de vulnérabilité des nappes phréatique de la région de Saida, en Algérie, avec l'aide des systèmes d'information géographique. MS. thesis. Canada: MONCTON University.

Chowdhury A, Jha MK, Chowdary VM, *et al*. 2009. Integrated remote sensing and GIS-based approach for assessing groundwater potential in West Medinipur District, West Bengal, India. International Journal of Remote Sensing, 30(1): 231-250.

Dahmani MN. 2016. Etude hydrologique e hydro-géologique du Bassin versant de l'Oued Saida, Magister thesis, University of d'Oran 2, Algeria. https://ds.univ-oran2.dz:8443/jspui/handle/123456789/458

Das B, Pal SC. (2019). Combination of GIS and fuzzy-AHP for delineating groundwater recharge potential zones in the critical Goghat-II block of West Bengal, India. HydroResearch, 2: 21-30.

Djidi K, Bakalowicz M, Benali AM. 2008. Mixed, classical and hydrothermal karstification in a carbonate aquifer: Hydrogeological consequences. The case of the Saida aquifer system, Algeria. Comptes Rendus Geoscience, 340(7): 462-473.

Döell P, Hoffmann-Dobrev H, Portmann F, *et*

al. 2012. Impact of water withdrawals from groundwater and surface water on continental water storage variations. Journal of Geodynamics, 59: 143-156.

Edet AE, Okereke CS, Teme SC, *et al*. 1998. Application of remote sensing data to groundwater exploration: A case study of the Cross River State, South Nigeria. Hydrogeology Journal, 6(3): 394-404.

Field CB, Barros VR, Dokken DJ, *et al*. 2014. IPCC Climate change 2014: Impacts, adaptation and vulnerability. Part A: Global and sectoral aspects. Contribution of working group II to the Fifth Cambridge, United Kingdom and NewYork, NY, USA: Cambridge University Press: 1132.

Gdoura K, Anane M, Jellali S. 2015. Geospatial and AHP multicriteria analyses to locate and rank suitable sites for groundwater recharge with reclaimed water. Resources, Conservation and Recycling, 104: 19-30.

Gebru H, Gebreyohannes T, Hagos E. 2020. Identification of groundwater potential zones using analytical hierarchy process (AHP) and GIS-remote sensing integration, the Case of Golina River Basin, Northern Ethiopia. International Journal, 9(1): 3289-3311.

Ghosh D, Mandal M, Karmakar M, *et al*. 2020. Application of geospatial technology for delineating groundwater potential zones in the Gandheswari Watershed, West Bengal. Sustain. Water Resour Manag, 6: 14. https://link.springer.com/article/10.1007/s40899-020-00372-0

Hachem AM, Ali E, El Ouali Abdelhadi EHA, *et al*. 2015. Using remote sensing and GIS-Multicriteria decision analysis for groundwater potential mapping in the Middle Atlas Plateaus, Morocco. Research Journal of Recent Sciences, 4(7): 1-10.

Hanquiez V, Coutelier C, Pierson J. 2014. Introduction a l'analyse spatiale sur ArcGis for Desktop 10.2. Université de Bordeaux et CNRS. http://vincent.hanquiez.free.fr/Images/Hanquiez_Formation_ArcGIS10.2_IntroAS.pdf

Hennequi M. 2010. Spatialization of modeling data by Krigeage. Strasburg University: 7. https://dumas.ccsd.cnrs.fr/dumas-00520260/document

Huisman O, Rolf De by. 2009. Principles of geographic information systems-an introductory text book, serie 1. The interna-tional institute for geo-information science and earth observation. Netherlands: ITC: 1-441.

Isaaks EH, Srivastava RM. 1989. An introduction to applied geostatistics. New York: Oxford University Press.

Jha MK, Chowdary VM, Chowdhury A. 2010. Groundwater assessment in Salboni Block, West Bengal (India) using remote sensing, geographical information system and multicriteria decision analysis techniques. Hydrogeology Journal, 18(7): 1713-1728. https://doi.org/10.1007/s10040-010-0631-z

Jordan G, Meijninger BML, Hinsbergen DJJV, *et al*. 2005. Extraction of morphotectonic features from DEMs: Development and applications for study areas in Hungary and NW Greece. International Journal of Applied Earth Observation and Geoinformation, 7(3): 163-182.

Kanohin F, Saley MB, Aké GE, *et al*. 2012. Apport de la télédétection et des SIG dans l'identification des ressources en eau souterraine dans la région de Daoukro (Centre- Est de la Côte D'Ivoire). Journal of Innovation and Applied Studies, 1(1): 35-53.

Kessar C, Benkesmia Y, Blissag B, *et al*. 2020. Gis based analytical hierarchical process for the assessment of groundwater potential zones in Wadi Saida Watershed (NW-ALGERIA). 2020 Mediterranean and Middle-East Geoscience and Remote Sensing Symposium (M2GARSS). IEEE: 277-280.

Kettab A. 2001. Les ressources en eau en Algérie: stratégies, enjeux et vision. Desalination, 136(1-3): 25-33.

Klaus GD. 2013. Implementing the analytic hierarchy process as a standard method for multi-criteria decision making in corporate enterprises-a new AHP excel template with multiple inputs. Proceedings of the International Symposium on the Analytic Hierarchy Process: 1-10.

Koita M, Jourde H, Ruelland D, *et al*. 2010. Cartographie des accidents régionaux et identification de leur rôle dans l'hydrodynamique souterraine en zone de socle. Cas de la région de Dimbokro-Bongouanou (Côte

d'Ivoire). Hydrological Sciences Journal, 55(5): 805-820.

Koudou A, Assoma TV, Adiaffi B, *et al*. 2014. Analyses statistique et géostatistique de la fracturation extraite de l'imagerie ASAR ENVISAT du SUD-EST de la Côte d'Ivoire. Larhyss Journal, 20: 147-166.

Kumar T, Gautam K, Kumar T. 2014. Appraising the accuracy of GIS based multicriteria decision making technique for delineation of groundwater potential zones. Water Resources Management, 28: 4449-4466.

Le Page M, Berjamy B, Fakir Y, *et al*. 2012. An integrated DSS for groundwater management based on remote sensing. The case of a semi-arid aquifer in Morocco. Water Resources Management, 26(11): 3209-3230.

Leroux R. 2007. Définition et application d'une méthodologie pour l'étude de la propagation d'états de mer en milieu côtier. http://web.univ-ubs.fr/lmba/frenod/IMG/pdf/Rap-StagRomain.pdf. (in French)

Machiwal D, Jha MK, Mal BC. 2011. Assessment of groundwater potential in semi-arid region of india using remote sensing, GIS and MCDM Techniques. Water Resources Management, 25(5): 1359-1386.

Magesh NS, Chandrasekar N, Soundranayagam JP. 2012. Delineation of groundwater potential zones in Theni. District, Tamil Nadu, using remote sensing, GIS and MIF techniques. Geoscience Frontiers, 3(2): 189-196.

Maity DK, Manda S. 2017. Identification of groundwater potential zones of the Kumari river Basin, India: An RS and GIS based semi-quantitative approach. Environ Dev Sustain, 21: 1013-1034.

Malczewski J. 1999. GIS and Multicriteria decision analysis. Wiley, United States of America: 177-192.

Medjber A, Berkane F. 2016. Quantification et évolution du Bilan de la nappe karstique de Saida (Nord-Ouest De l'Algérie). Journal Scientifique Européen, 12(9): 349. (in French)

NAHR. 2008. The 1/200 000 geological map of northern Algeria.

NAHR. 2014. Five Stations Rainfall Data.

Nas B. 2009. Geostatistical approach to assessment of spatial distribution of groundwater quality. Polish Journal of Environmental Studies, 18(6): 1073-1082.

Nithyaa CN, Srinivas Y, Magesh NS, *et al*. 2019. Assessment of groundwater potential zones in Chittar basin, Southern India using GIS based AHP technique. Remote Sensing Applications: Society and Environment, 5: 1-15.

Nouayti A, Khattach D, Hilali M, *et al*. 2019. Mapping potential areas for groundwater storage in the High Guir Basin (Morocco): Contribution of remote sensing and geographic information system. Journal of Groundwater Science and Engineering, 7(4): 309-322.

Nouayti N, Khattach D, Hilali M. 2017. Potential areas mapping for the groundwater storage in the high Ziz Basin (Morocco): Contribution of remote sensing and geographic information system. Bulletin de l'Institut Scientifique, Rabat, Section Sciences de la Terre, 39: 45-57.

Ould Cherif Ahmed A, Nagasawa R, Hattorin K, *et al*. 2008. Identification of groundwater potential areas in arid land using remote sensing and GIS: A case study for the Adrar region of northern Mauritania. Sand Dune Research, 55(1): 1-11.

Pankaj KS, Amit KB. 2006. Groundwater assessment through an integrated approach using remote sensing, GIS and resistivity techniques: A case study from a hard rock terrain. International Journal of Remote Sensing, 27(20): 4599-4620.

Pitaud G. 1973. Etude hydrogéologique pour la mise en valeur de la vallée de l'oued Saïda, DEMRH: 54-55. (in French)

Prasad RK, Mondal NC, Banerjee P, *et al*. 2008. Deciphering potential groundwater zone in hard rock through the application of GIS. Environmental Geology, 55: 467-475.

Pretorius JPG, Partridge TC. 1974. Analysis of angular a typicality of lineaments as aid to mineral exploration. Journal of South African Institute of Mining and Metallurgy, 74(10): 367-369.

Rahmati O, Samani AN, Mahdavi M, *et al*. 2015. Groundwater potential mapping at Kurdistan region of Iran using analytic hierarchy process and GIS. Arabian Journal of Geosciences, 8: 7059-7071.

Rajasekhar M, Sudarsana Raju G, Sreenivasulu Y, *et al*. 2019. Delineation of groundwater potential zones in semi-arid region of Jilledubanderu river basin, Anantapur District, Andhra Pradesh, India using fuzzy logic, AHP and integrated fuzzy-AHP approaches. Hydro Research, 2: 97-108.

Rao BV, Briz-Kishore BH. 1991. A methodology for locating potential aquifers in a typical semi-arid region in India using resistivity and hydrogeologic parameters. Geoexploration, 27(1-2): 55-64.

Rilo RSA, Doni PEP, Lucas DS. 2019. Delineation of groundwater potential zones using remote sensing, GIS, and AHP techniques in southern region of Banjarnegara, Central Java, Indonesia, In: Proc. SPIE 11311, Sixth Geoinformation Science Symposium. Doi: 10.1117/12.2548473

Saaty TL. 1980. The analytic hierarchy process: Planning, priority setting, resource allocation. New York: McGraw-Hill: 340.

Sander P. 2007. Lineaments in groundwater exploration: A review of applications and limitations. Hydrogeology Journal, 15(1): 71-74.

Saprikhine O, Riabenko V. 1978. Rapport sur les résultants des recherches systématiques et levé géologique à 1/50 000 effectué en 1978 par l'équipe dans le périmètre de la feuille n°304 (Saida). (in French)

Sekar I, Randhir TO. 2007. Spatial assessment of conjunctive water harvesting potential in watershed systems. Journal of Hydrology, 334(1-2): 39-52.

Senanayake IP, Dissanayake DMDOK, Mayadunna BB, *et al*. 2015. An approach to delineate groundwater recharge potential sites in Ambalantota, Sri Lanka using GIS techniques. Geoscience Frontiers, 7(1): 115-124.

Shekhar S, Pandey AC. 2014. Delineation of groundwater potential zone in hard rock terrain of India using remote sensing, geographical information system (GIS) and analytic hierarchy process (AHP) techniques. Geocarto International, 30(4): 402-421.

Suja Rose RS, Krishnan N. 2009. Spatial analysis of groundwater potential using remote sensing and GIS in the Kanyakumari and Nambiyar basins, India. Journal of the Indian Society of Remote Sensing, 37: 681-692. Doi: 10.1007/s12524-009-0058-y

Wondifraw N, Binyam TH, Tilahun A. 2019. Mapping of groundwater potential zones using sentinel satellites (-1 SAR and -2A MSI) images and analytical hierarchy process in Ketar Watershed, Main Ethiopian Rift. Journal of African Earth Sciences, 160: 1-17.

WWDR. 2019. UN World Water Development Report 2019: Leaving No One Behind. The United Nations Educational, Scientific and Cultural Organization.

Yles F. 2014. Modélisation pluie-débit et transport solide dans le bassin versant de l'oued Saida. Ph.D. thesis, Algeria: Abou Bakr Belkaid University. (in French)